お茶の水女子大学自然科学報告　第74巻　第1号、第2号
Natural Science Report, Ochanomizu University, Vol. 74, No. 1, No. 2 (2024)

Periodic structure appearing in rotating thermal fluid in uniform flow

Ibuki Fujisawa, Tetsuo Deguchi, Tetuya Kawamura

<Abstract>

In this study, the heat convection generated by a square-shaped heat source placed in a rotating fluid is investigated by numerical simulation. The incompressible Navier-Stokes equations with the Bousinesq approximation and the advection-diffusion equation for temperature are taken as the basic equations. The Coriolis force is added as an external force. These equations are solved by the fractional step method, and the nonlinear terms of the Navier-Stokes equations are approximated by the third-order upstream finite difference method so that calculations can be stably performed even at high Reynolds numbers. As a result, in some region of inflow velocity (Reynolds number), buoyancy (Grashof number), and Coriolis force (Rosby number), a stable periodic flow structure appears downstream of the heat source. Moreover, the parameter dependence of the flow and the mechanism of periodic structure generation are investigated.

1. Introduction

In a fluid flow, even a region of simple geometry can create a regular pattern that is difficult to imagine from that geometry. For example, in a flow around a cylinder, a Karman vortex street is created behind the cylinder within a certain Reynolds number range. Fluids that are hotter than their surroundings rise under buoyancy, and a great variety of flows arise from this simple principle. Among them, the following are examples of regular patterns. Between two horizontally arranged flat plates, the fluid between the plates can generate regular roll-shaped vortex streets when the lower plate is heated. Meandering westerly winds are large-scale waves associated with the rotation of the Earth, and are thought to be Rossby waves that appear in rotating fluids.

There are many studies on flows with characteristic patterns such as Karman vortices and thermal convection, and the results are introduced in many fluid mechanics textbooks 1). Laboratory experiments on meandering westerly winds were conducted by filling water between two cylinders, creating a temperature difference between the inner and outer cylinder surfaces to generate convection, and rotating the entire apparatus around an axis. At this time, various wave patterns are obtained 2). This phenomenon is also investigated in detail by numerical simulations 3).

In this study, we consider a different situation from the above as a flow in a simple

geometry where buoyancy and Coriolis forces play an important role. That is, in a rectangular parallelepiped area, a square heat source is placed on the bottom surface to cause convection, and the entire area is assumed to be rotating where the flow is allowed to enter from one side. There are simulations and experimental studies as a model of a fire tornado when there is no lateral flow. For example, when heat convection is generated in a circular or ring-shaped heat source, an upward flow is generated above the heat source, and at that time, a flow is generated from the surroundings toward the heat source. If the region is rotating, each fluid will gather above the heat source with angular momentum 4). Since angular momentum is conserved, concentrating on a region will increase the rotation. This is thought to be one of the mechanisms that generate tornadoes. This simulation assumes axial symmetry because it is a study of the era when the power of computers was low. Since then, the shape of the heat source has been changed to make three dimensional flow and the effect on tornado formation has been studied in detail 5) 6) 7).

This study is an extension of such fire tornado research, and is also related to investigating the behavior of fire tornado when the wind is blowing.

2. Numerical Method

Since the purpose of this study is to investigate the effects of buoyancy and Coriolis forces on the flow, the basic equations are the Navier-Stokes equation in rotational coordinate system with the Bousinesq approximation and the advection-diffusion equation for temperature.

$$\frac{\partial u}{\partial x}+\frac{\partial v}{\partial y}+\frac{\partial w}{\partial z}=0 \tag{1}$$

$$\frac{\partial u}{\partial t}+u\frac{\partial u}{\partial x}+v\frac{\partial u}{\partial y}+w\frac{\partial u}{\partial z}=-\frac{\partial p}{\partial x}+\frac{1}{Re}\left(\frac{\partial^2 u}{\partial x^2}+\frac{\partial^2 u}{\partial y^2}+\frac{\partial^2 u}{\partial z^2}\right)+\frac{1}{R_0}v \tag{2}$$

$$\frac{\partial v}{\partial t}+u\frac{\partial v}{\partial x}+v\frac{\partial v}{\partial y}+w\frac{\partial v}{\partial z}=-\frac{\partial p}{\partial y}+\frac{1}{Re}\left(\frac{\partial^2 v}{\partial x^2}+\frac{\partial^2 v}{\partial y^2}+\frac{\partial^2 v}{\partial z^2}\right)-\frac{1}{R_0}u \tag{3}$$

$$\frac{\partial w}{\partial t}+u\frac{\partial w}{\partial x}+v\frac{\partial w}{\partial y}+w\frac{\partial w}{\partial z}=-\frac{\partial p}{\partial z}+\frac{1}{Re}\left(\frac{\partial^2 v}{\partial x^2}+\frac{\partial^2 v}{\partial y^2}+\frac{\partial^2 w}{\partial z^2}\right)+\frac{Gr}{Re^2}T \tag{4}$$

$$\frac{\partial T}{\partial t}+u\frac{\partial T}{\partial x}+v\frac{\partial T}{\partial y}+w\frac{\partial T}{\partial z}=\frac{1}{RePr}\left(\frac{\partial^2 T}{\partial x^2}+\frac{\partial^2 T}{\partial y^2}+\frac{\partial^2 T}{\partial z^2}\right) \tag{5}$$

Here, Re is the Reynolds number, Gr is the Grashof number, and Ro is the Rossby number, and these parameters are varied to see the effect on the flow. Pr is the Prandtl number, which is fixed at 0.71 in this study because air is assumed. These equations are

solved by using the fractional step method, which solves pressure and velocity separately. The nonlinear term of the Navier-Stokes equation is approximated by the third-order accuracy upstream difference, which can be calculated stably even at high Reynolds numbers. On the other hand, at grid points one inside the boundary, the first-order accuracy upstream difference is employed in order to avoid using virtual grid points outside of the region, and the non-linear term of the heat advection-diffusion equation is also approximated by the first-order accuracy upstream difference in order to further improve the stability.

The calculation area is a rectangular parallelepiped, and the shape of the heat source is a square. When the length of one side of the heat source is 1, the size of the area is 3.2 in the flow direction, 3.2 in the span direction, and 1.6 in the height direction. The grid is shown in Figure 1 and is evenly spaced (width 0.04) horizontally and vertically near the heat source, while non-uniform grids are used in which the spacing increases as the distance from the heat source increases in order to reduce the total number of grids. The number of grids used in this calculation is 100 in the horizontal two directions and 50 in the vertical direction, for a total of 500,000 points.

As boundary conditions for the velocity, a uniform flow velocity is given on the surface on the inflow side, a flow velocity of 0 (no-slip condition) on the lower surface, and an outflow condition (the normal derivative to the boundary is 0) on the other surfaces. As for the pressure, the normal derivative to each surface is set to 0. As an initial condition, the fluid is assumed to be rest except for the inflow surface, and the bottom surface is also suddenly heated by a heat source.

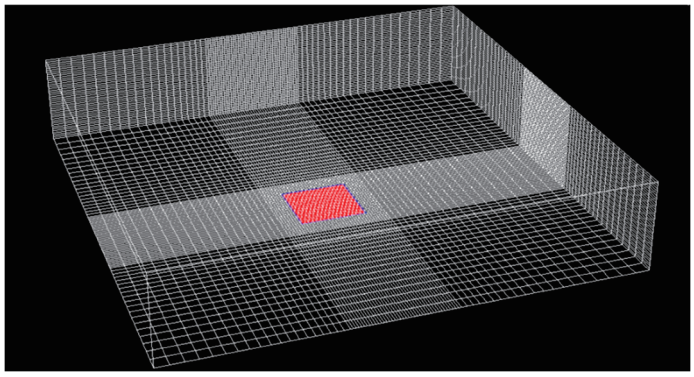

Fig.1 The calculation area and position and size of the heat source

3. Results

As a typical calculation example, the results of $Re = 2000, Gr/Re^2 = 1.0, R_0 = 1.5$ are shown first. In this study, Re is based on inflow velocity and length of one side of the

heat source. Hereinafter, the number of steps will be used instead of non-dimensional time when the time interval Δt between steps is 0.01. FIG. 2 shows the locations of the temperature observation points. FIG. 3 shows the number of steps from the start of calculation on the horizontal axis and the temperature at each observation point on the vertical axis. Focusing on the initial stage (up to the 500 step), the number of time steps at which the temperature rises sharply differs and it becomes large as the distance from the heat source increases. Strong fluctuations in the elevated temperature indicate unsteady flow. After that, it goes through a transitional period (from 3300 step to 5200 step) and reaches periodic stage at each observation point. This means that the flow becomes entirely periodic.

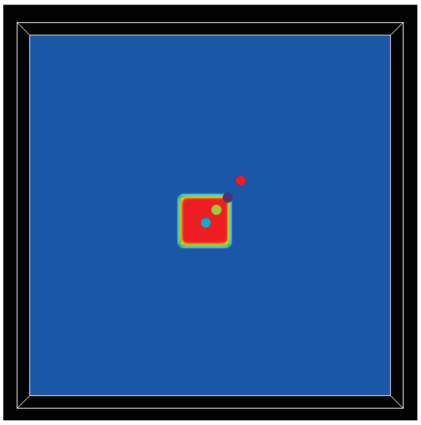

Fig.2 Locations of the temperature observation points

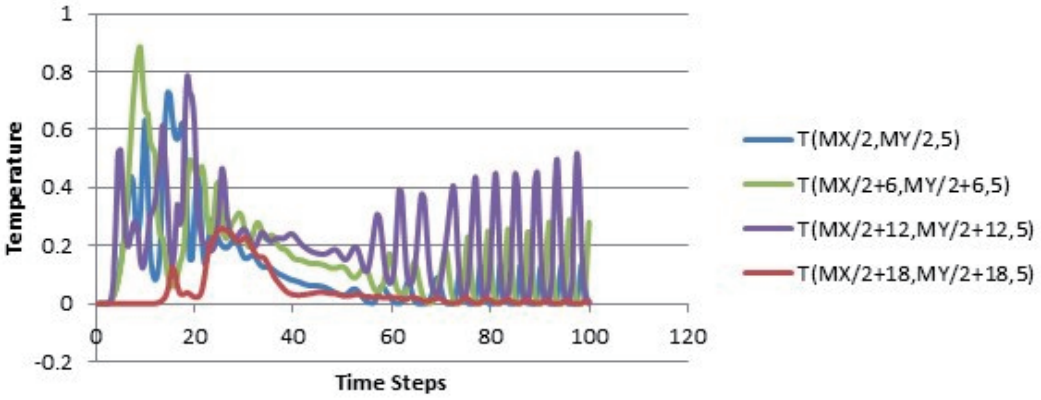

Fig. 3 Relationship between number of time steps and temperature at each observation point ($Re = 2000,\ Gr/Re^2 = 1.0, R_0 = 1.5$)

MX : Number of grid points in the X-direction

MY : Number of grid points in the Y-direction

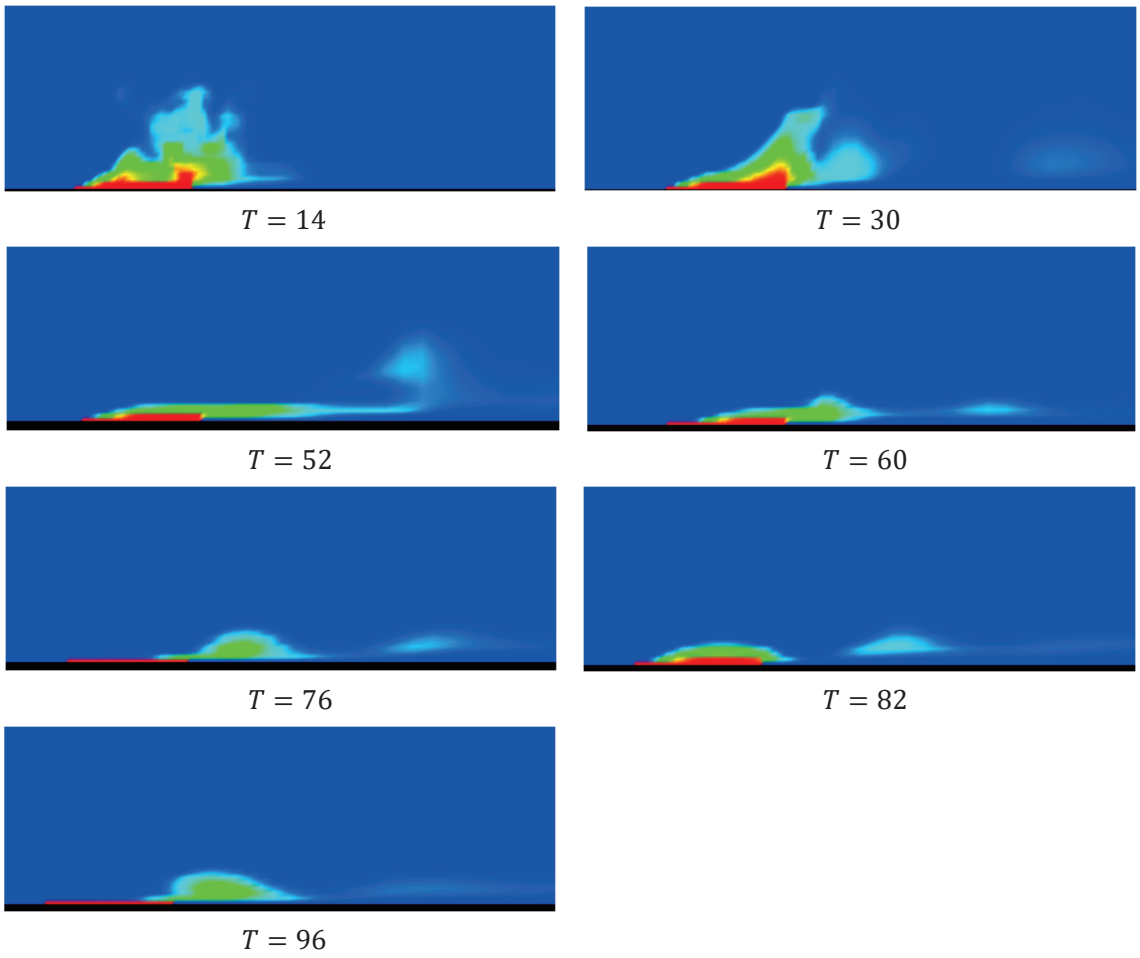

Fig.4 Temperature distribution in the central cross section at typical time steps ($Re = 2000,\ Gr/Re^2 = 1.0, R_0 = 1.5$)

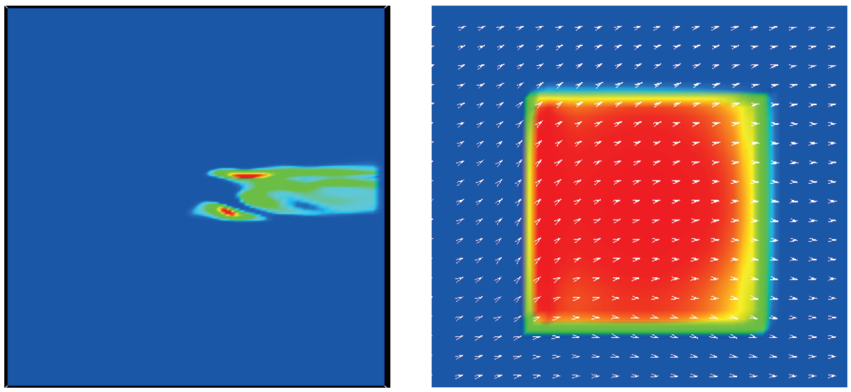

Fig. 5 Temperature distribution and velocity vector in horizontal cross section (Distance 0.2 from the bottom surface, 6800 step)

FIG. 4 shows (in chronological order) the temperature distribution at a typical step in the x-z plane across to the center of the heat source. FIG. 5 shows temperature

distribution and velocity vectors in a horizontal cross section (distance 0.2 from the bottom surface)

Next, the results of $Re = 40,\ Gr/Re^2 = 1.0,\ R_0 = 0.75$ are shown.

FIG. 6 shows results corresponding to FIG. 3, where the horizontal axis indicates time and the vertical axis indicates temperature at the same observation points as in FIG.3. In this case, there is no initial temperature fluctuation as seen in FIG. 3, and the oscillation gradually attenuates after having a peak near $T = 8 - 10$, approaching a constant value. FIG. 7 shows the temperature distribution at 400, 800, 1200, 1600, 2000, 4400, 8400, 10000 steps in the central cross section corresponding to FIG 3.

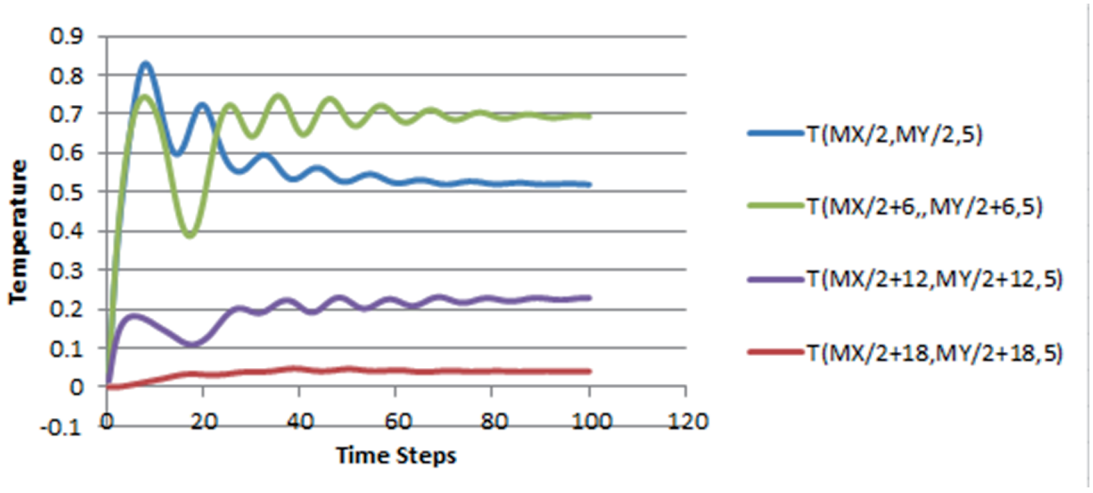

Fig. 6 Relationship between number of time steps and temperature at each observation point ($Re = 40, Gr/Re^2 = 1.0, R_0 = 0.75$)

MX : Number of grid points in the X-direction

MY : Number of grid points in the Y-direction

As is shown, it is found that there are two cases, one in which the oscillation persists and the other in which the oscillation attenuates, depending on the parameters. Next, it is examined what kind of flow patterns appear. FIG. 8 is a map with the Coriolis force (Rosby number) on the horizontal axis and the Reynolds number on the vertical axis.

The numbers inside the red circles represent the elapsing time at which the vibrating pattern appears after the initial state. When the flow is oscillating, the period and the amplitude also change depending on the parameters. To see the tendency, the period and the amplitude are shown in Table 1 and Table 2, respectively, where the Reynolds number is in the vertical column and Coriolis forces is in the horizontal column.

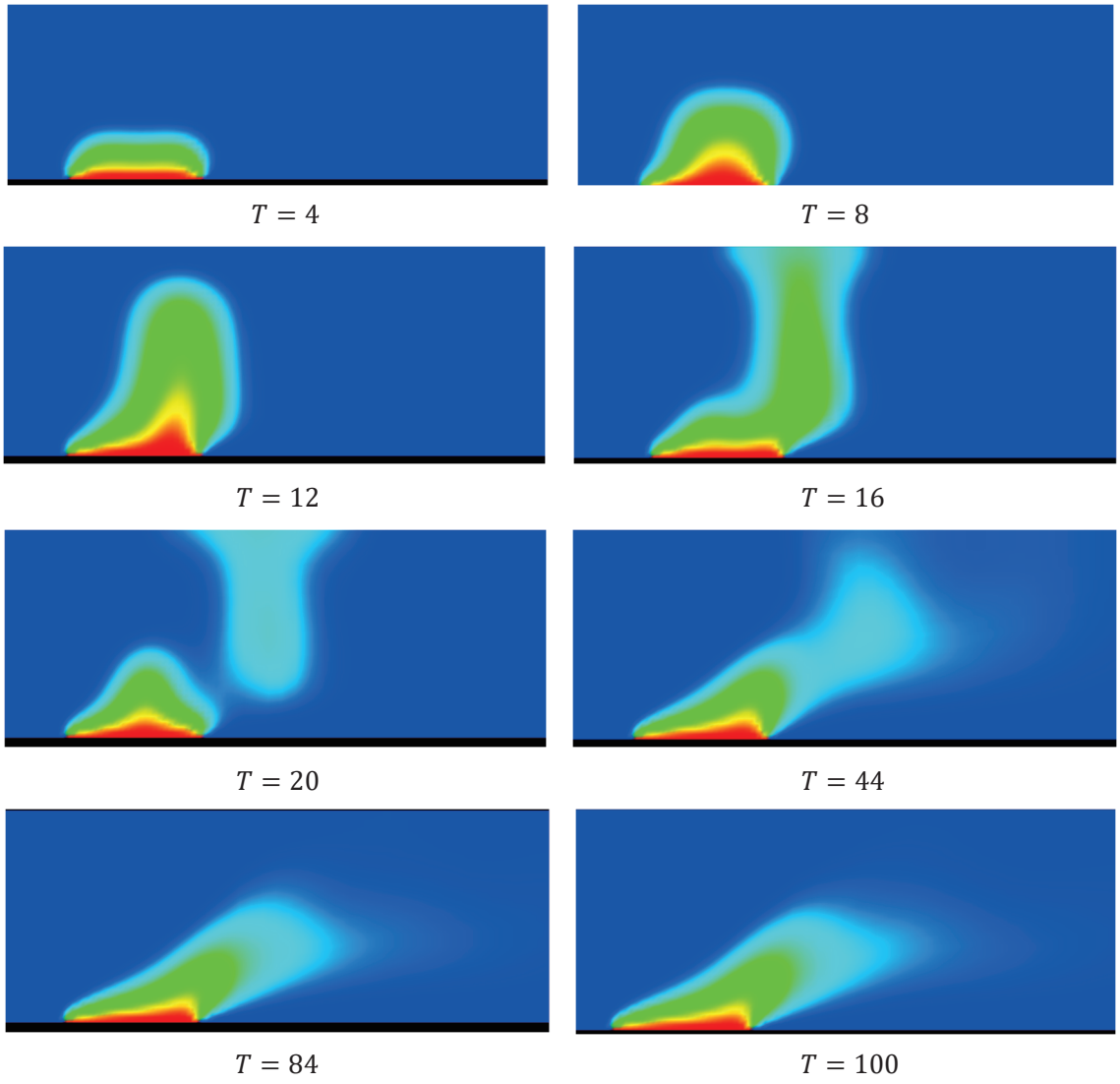

Fig. 7 Temperature distribution in the central cross section at various time steps ($Re = 40, Gr/Re^2 = 1.0, R_0 = 0.75$)

Next, the effect of the magnitude of the buoyant force on the period is investigated. The Reynolds number is fixed at 2000 and calculations are performed with varying buoyancy and Coriolis forces. In FIG. 11 to 13, the horizontal axis represents the magnitude of buoyancy, and the vertical axes represent the time at which vibration starts, the period of vibration, and the amplitude of vibration, respectively.

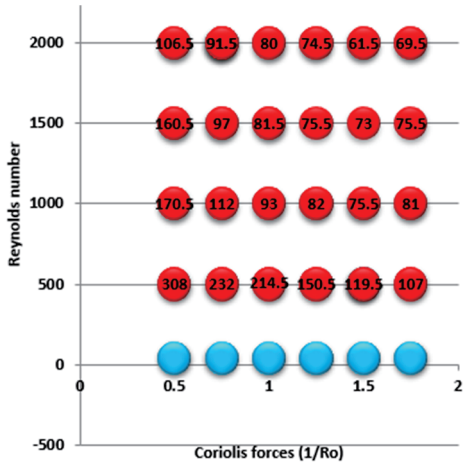

Fig.8 Starting time of occurrence of oscillation and the pattern for various Rosby and Reynolds numbers

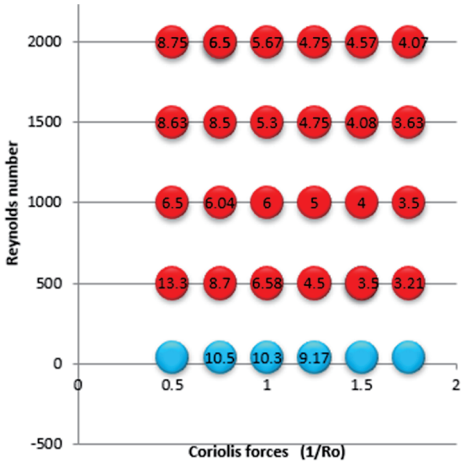

Fig.9 Period of oscillation and the pattern for various Rosby and Reynolds numbers

Coriolis force (1/Ro) / Reynolds number	0.5	0.75	1.0	1.25	1.5	1.75
40		10.5	10.3	9.17		
500	13.3	8.7	6.58	4.5	3.5	3.21
1000	6.5	6.04	6	5	4	3.5
1500	8.63	8.5	5.3	4.75	4.08	3.63
2000	8.75	6.5	5.67	4.75	4.57	4.07

Table 1 Period of oscillation and the pattern for various Rosby and Reynolds numbers

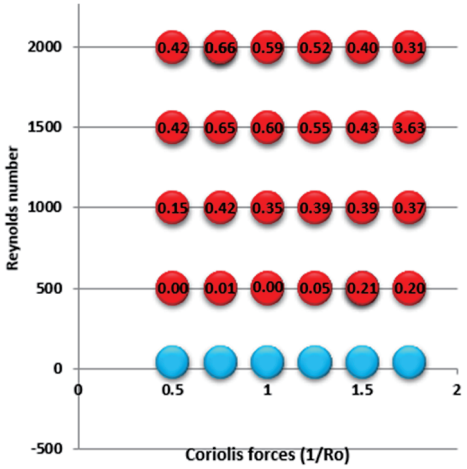

Fig.10 Period of oscillation and the pattern for various Rosby and Reynolds numbers

Reynolds number \ Coriolis force (1/Ro)	0.5	0.75	1.0	1.25	1.5	1.75
40						
500	0.00	0.01	0.00	0.05	0.21	0.20
1000	0.15	0.42	0.35	0.39	0.39	0.37
1500	0.42	0.65	0.60	0.55	0.43	0.33
2000	0.42	0.66	0.59	0.52	0.40	0.31

Table 2 Amplitude of oscillation and pattern for various Rosby and Reynolds numbers

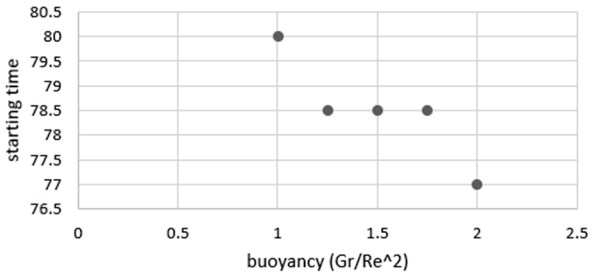

Fig. 11 Correlation between buoyancy and starting point of oscillation

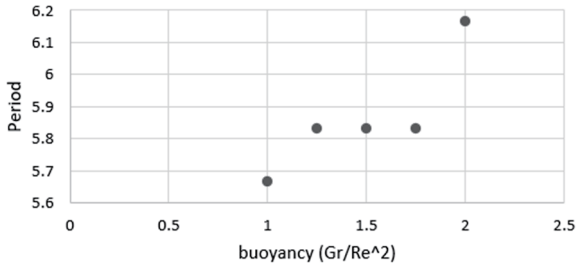

Fig.12 Correlation between buoyancy and period of oscillation

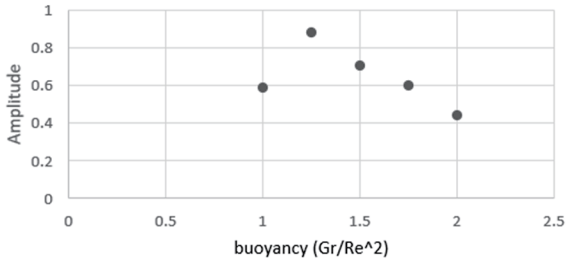

Fig. 13 Correlation between buoyancy and amplitude of oscillation

4. Discussion

Without uniform flow, there exists an upward flow from the heat source, but with uniform flow, the heated portion would sway downstream. However, this alone cannot explain periodic fluctuations downstream. On the other hand, without uniform flow and with the Coriolis force, the upward flow has rotation and is more concentrated and more stable than without Coriolis force. In other words, due to the influence of the Coriolis force, the hot spot is concentrated in a narrow area near the center compared to the case without the Coriolis force. This portion (warm air spot) grows larger as time going on, but if there is a uniform flow, once it reaches a certain size, it will be washed away by the uniform flow.

As a result, the temperature in the vicinity of the heat source decreases, and by the same process, a hot spot is created and grown and reflowed. This means a periodic structure appears.

It is considered that the stronger the rotation, the more easily the warm air spot is generated. Therefore, in FIG. 8, the time at which the periodic structure starts to appear becomes earlier as the Coriolis force increases .On the other hand, it is thought that the smaller the Reynolds number, the greater the diffusion effect and the more the heat convection is suppressed. As a result, the smaller the Reynolds number, the later the start time and when it becomes even smaller, the periodic structure disappears (blue circles in FIG. 8).

The period in the periodic structure is mainly affected by the Coriolis force, and the larger the Coriolis force, the shorter the period. The reason is thought to be as follows; the larger the Coriolis force, a warm air spot is more easily formed, and it is generated immediately after it is swept away by the current.

Table 2 shows that the amplitude increases as the Coriolis force decreases, except for small Reynolds numbers (500) and small Coriolis forces (0.5). Large amplitude means that the temperature fluctuations are large, and thus well-heated air passes by the

observation point without much diffusion. If the Coriolis force is small, it takes a long time to generate a warm spot, and as a result it is thought that the air is sufficiently warmed. When the Reynolds number is small, the heat is diffused and the amplitude becomes small. Above 1500 the effect of diffusion becomes less pronounced.
From FIG. 11 and 10, the buoyancy force has little effect on the period and onset time in the periodic structure of the flow. From FIG.11 on the other hand, except for the case where the buoyancy is 1, the smaller the buoyancy, the larger the amplitude. This is thought to be due to the fact that the smaller the buoyancy, the convection becomes weaker, and the longer the warm air spot stays near the heat source.

5. Summary

In this study, a square heat source is placed on a part of the lower surface of a rectangular parallelepiped area to generate heat convection, and a uniform flow flows in from one side, and the entire area is rotated. The flow in this situation is investigated by numerical simulation. This is a simple model of how a fire tornado behaves when the wind is blowing. The basic equation is the incompressible Navier-Stokes equation with the Bousinesq approximation. The Coriolis force is added as the external force. The nonlinear term of the Navier-Stokes equation is approximated by the third-order accuracy upstream difference so that the calculation can be stably performed even at a high Reynolds number.

The parameters governing the flow are the wind speed of the uniform flow (Reynolds number Re), the buoyancy due to the temperature difference between the heat source and the surrounding fluid (Grashof number Gr or Rayleigh number Ra), and the rotation relative to the size of the heat source and the speed of the uniform flow (Rosby number Ro).

As a result of the simulation, for example, when $Re = 2000, Gr = 1.0, Ro = 1.5$, a clear periodic flow structure appeared in the downstream part of the heat source while it does not appear when $Re = 40, Gr = 1.0, R_0 = 0.75$.

When investigating the time change of the temperature at a fixed point downstream, it is found that the flow changed to a clear periodic flow after a certain period of time, although it is turbulent-like flow at first. It is suggested that this phenomenon is caused by the balance of downstream advection effect by uniform flow, rising effect by buoyancy, and stabilizing effect by Coriolis force. Then, these three parameters are systematically changed to examine the effects of the parameters on the periodicity.

As a result, it is found that the larger the Coriolis force and the larger the Reynolds number, the faster the transition to the periodic structure and the shorter the period.

Furthermore, it is found that the periodic structure does not appear when the Reynolds number is small, and that the difference in the magnitude of the buoyancy force has a smaller effect on the periodic structure than the other two parameters.

Calculations with more grid points, increasing the number of cases for parameter studies, and conducting theoretical analyzes on the structure and the transition are the future works.

References

1) D.J.Tritton: Physical Fluid Dynamics 2nd. Ed. OXFORD SCIENCE PUBLICATIONS (1988)

2) K.Kikuchi, M.Uryu. and K. Kitabayashi: Introduction to experimental meteorology, the second term meteorological promenade, Tokyodo Press. 103-143 (1988)

3) Y.Kawazu, Y.Nagata and T.Kawamura: Numerical simulation of flow between two rotating coaxialcircular cylinders having different temperature, Natural Science Report, Ochanomizu University, V ol. 69, No. 1, No. 2 (2019)

4) K.Kuwahara and Y.Oshima: Thermal Convection Caused by Ring-Type Heat Source, Journal of Physical Society of Japan, Vol. 51 No.11 pp.3711-3719 (1982)

5) M.Kan, T.Kawamura and R.Iwatsu: Numerical Simulation of the Heat Convection by Using the Low-Mach Number Approximation , Trans. JSME Vol. 65 No. 629, pp. 108-115 (1999)

6) S.Komurasaki,T.Kawamura and K.Kuwahara: Vortex Breakdown in Fire Tornado, Theoretical and applied Mech. Vol.48, pp. 331-338(1999)

7) S.Komurasaki, T.Kawamura and K.Kuwahara: Simulation of Thermal Convection in a Stratified Fluid Flow, AIAA paper 2002-0877, pp.1-10 (2002)

Ibuki Fujisawa
Email: g1920215@outlook.jp

Tetsuo Deguchi
Email: deguchi@phys.ocha.ac.jp

Tetuya Kawamura
Email: kawamura@is.ocha.ac.jp